sidered to be "inert." Nevertheless, a degree of hybridization of s and p orbitals would be favored if the energy so expended were counterbalanced by electrostatic stabilization as suggested by Orgel,[14] or through overlap of the resulting hybrids to form bonding orbitals. If we allow hybridization of bismuth s and p_z orbitals on $Bi_6(OH)_{12}^{6+}$ (z is taken as the direction on each bismuth toward the center of the cage), the resulting hybrids would be favorably oriented for mutual overlap. They would form a bonding set of six molecular orbitals, inside the Bi_6 cage, in which the twelve bismuth valence electrons could be delocalized, and a corresponding antibonding set outside the cage.

The bismuth p_x and p_y orbitals would then be left for bonding with the hydroxyl oxygens. Twelve bonding molecular orbitals would thus be available for 24 of the hydroxyl electrons. Two filled orbitals on each oxygen would be left nonbonding. This arrangement is equivalent to a set of twelve three-center O–Bi–O bonds. The predicted average metal–oxygen bond order is one-half, and this may explain the somewhat low value for the Bi–O stretching constant. Twelve three-center metal–ligand bonds are also called for in the equivalent orbital scheme for the $Ta_6Cl_{12}^{2+}$ cage proposed by Kettle.[15] However his use of eight face-centered orbitals for metal–metal bonding is inapplicable to Bi(III).

A possible energy level scheme based on these considerations is sketched out in Figure 2. Here bismuth ions (A) are allowed to hybridize individually (B), come together in an octahedral array (C), and then combine with hydroxyl ions (D). The ordering of energy levels is far from unambiguous, but it seems profitless at this time to undertake a quantitative calculation. Since the 6p–6d separation in Bi(III) is not much larger than the 6s–6p separation,[13] a more complete description would have to consider mixing in of bismuth d orbitals as well. However our purpose here is merely to indicate that weak bismuth–bismuth bonding may be a reasonable feature of the electronic structure of $Bi_6(OH)_{12}^{6+}$.

Acknowledgment.—We are indebted to Professors Niel Bartlett and William DeW. Horrocks for invaluable discussions of our results. This work made use of computer facilities supported in part by National Science Foundation Grant NSF-GP579.

(14) L. E. Orgel, *J. Chem. Soc.*, 3815 (1959).

(15) S. F. A. Kettle, *Theoret. Chim. Acta*, **3**, 211 (1965).

CONTRIBUTION FROM THE DEPARTMENT OF CHEMISTRY,
PRINCETON UNIVERSITY, PRINCETON, NEW JERSEY 08540

Vibrational Analysis for Polynuclear Hydroxylead(II) Complexes[1a]

BY VICTOR A. MARONI[1b] AND THOMAS G. SPIRO

Received June 13, 1967

The vibrational spectrum of $Pb_4(OH)_4^{4+}$ has been subjected to a normal coordinate analysis, based on a tetrahedral structure for this species, using the known Pb–Pb and Pb–O distances in solution. Agreement with experiment was readily obtained, but only if an attractive interaction between lead atoms was included in the force field. For the complex containing 1.33 hydroxides per lead, whose composition is probably $Pb_6(OH)_8^{4+}$, the presumption of an octahedral structure is supported by the observation of three low-frequency Raman bands at frequency ratios found to be characteristic of metal cages of cubic symmetry. A vibrational analysis based on this structure and the assumption that the Pb–Pb and Pb–O distances are the same as for $Pb_4(OH)_4^{4+}$ led to an excellent fit of the data with force constants similar to those used for $Pb_4(OH)_4^{4+}$. Evidence for lead–lead bonding in these complexes is provided by the anomalously high intensity observed for the low-frequency Raman bands attributable to the lead cages. A bonding scheme similar to that proposed[2] for $Bi_6(OH)_{12}^{6+}$ can be applied.

Introduction

The previous article[2] described a normal coordinate analyses for the $Bi_6(OH)_{12}^{6+}$ cuboctahedron. The main conclusion reached was that the Raman spectrum could best be understood on the basis of direct, if weak, bonding among the bismuth atoms. In the present work we continue our spectroscopic studies of hydroxymetal polyhedra, with an analysis of the vibrational spectra of polynuclear lead complexes, which were recently reported.[3] The results parallel those obtained for $Bi_6(OH)_{12}^{6+}$, Raman spectra again providing evidence for weak metal–metal bonding.

Lead(II) is isoelectronic with bismuth(III) and both hydrolyze to give soluble complexes, whose structures are however quite different. Bismuth produces the octahedral hexamer $Bi_6(OH)_{12}^{6+}$ while the main product of lead hydrolysis is a tetramer, $Pb_4(OH)_4^{4+}$. Its structure, as deduced by Esval[4] from solution X-ray scattering measurements, is a distorted cube consisting of lead and oxygen atoms arranged tetrahedrally, as shown in Figure 1. The Raman spectrum of per-

(1) (a) This investigation was supported by Public Health Service Grant GM-13498, from the National Institute of General Medical Sciences; (b) NASA Predoctoral Fellow.

(2) V. A. Maroni and T. G. Spiro, *Inorg. Chem.*, **7**, 183 (1968).

(3) V. A. Maroni and T. G. Spiro, *J. Am. Chem. Soc.*, **89**, 45 (1967).

(4) O. E. Esval, Thesis, University of North Carolina, 1962.

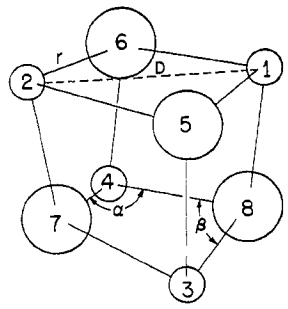

Figure 1.—Arrangement of lead atoms (small circles) and oxygen atoms (large circles) in the model assumed for $Pb_4(OH)_4^{4+}$. Parameters:[4] r = 2.57 Å, D = 3.81 Å, α = 84°, β = 96°.

chlorate solutions containing this complex and Raman and infrared spectra of crystals obtained from these solutions have been shown[3] to be qualitatively in accord with the tetrahedral structure. The present analysis sets this accord on a quantitative basis and throws light on the requisite force field.

Solutions can also be prepared which contain 1.33 hydroxyls per lead. These appear to contain an equilibrium mixture of $Pb_3(OH)_4^{2+}$ and $Pb_6(OH)_8^{4+}$ as indicated by Olin's[5] potentiometric and Esval and Johnson's[6] ultracentrifuge measurements. Raman spectra of saturated solutions and of the crystals obtained from them showed the same features[3] indicating the presence in both phases of the same structural unit. This is presumably the hexamer, whose formation is favored at high concentration. No structural information on this complex is available, but the Raman and infrared spectra could be interpreted[3] on the basis of the most symmetrical possible structure: one in which the six leads are arranged octahedrally, with the eight hydroxyls on the octahedral faces, analogous to the well-characterized complex $Mo_6Cl_8^{4+}$.[7] The present analysis strengthens this interpretation considerably.

Vibrational Analysis for $Pb_4(OH)_4^{4+}$

The observed Raman and infrared bands for $Pb_4(OH)_4^{4+}$ have been assigned[3] to symmetry classes on the basis of a tetrahedral structure. Hydrogen atoms were neglected and only the cage modes were considered. The two lowest frequency Raman bands, at 87 and 60 cm^{-1}, were assigned to F_2 and E modes, respectively, although there was no real basis for ruling out the reverse assignment. The latter in fact gives a more reasonable result in the normal coordinate analysis and is accepted here accordingly.

F and G matrices were constructed according to Wilson, Decius, and Cross,[8] using the interatomic distances reported by Esval.[4] Although Esval's measurements were made on solutions of $Pb_4(OH)_4^{4+}$, we have combined solution and solid spectral data, since more bands are resolved in the solid phase. Our justification for assuming that the same molecular parameters can be used for both solution and solid rests on the close agreement of the Raman bands which are well resolved in both phases. Calculation of the G matrix elements and solution of the secular equation with least-squares refinement of the force constants were carried out by computer, using programs SD-4064 and SD-4032, respectively, both of which have been developed by Schachtschneider.[9]

The internal coordinates are defined in Figure 1. As in the case of $Bi_6(OH)_{12}^{6+}$,[2] our initial approach was to use a force field containing a metal–oxygen stretching constant and bending constants for the two structural angles, adding on interaction constants as seemed necessary. However this approach was quite unsuccessful with $Pb_4(OH)_4^{4+}$. No adequate fit to the data was obtained, even when the number of independent force constants, of reasonable magnitude, was increased to seven (the number of frequencies observable).

When the force field was altered to include a metal–metal stretching constant in place of the bending constants, the calculation improved dramatically. A good fit of the seven frequencies was obtained with four force constants: the Pb–Pb and Pb–O stretching constants and two Pb–O stretch–stretch interaction constants. These constants are defined in Table I, which

TABLE I
NONZERO SYMMETRY F MATRIX ELEMENTS FOR $Pb_4(OH)_4^{4+}$ [a]

A_1

$F_{rr} = K + 2k' + 2k''$
$F_{DD} = D$

E

$F_{rr} = K - k' - k''$
$F_{DD} = D$

F_2

$F_{r(1)r(1)} = K$
$F_{r(2)r(2)} = K + k' + k''$
$F_{r(1)r(2)} = \sqrt{2}(k' - k'')$
$F_{DD} = D$

[a] Symbols: K, Pb–O stretching constant; D, Pb–Pb interaction; k', stretch–stretch interaction at the angle α; k'', stretch–stretch interaction at the angle β.

shows how they are combined in the symmetry F matrix elements. Table II lists the symmetry coordinates formed from the Pb–O and Pb–Pb internal coordinates. The results of this calculation are shown under the heading calculation I in Table III, which compares observed and calculated frequencies and lists the adjusted force constants. The discrepancies between the observed and calculated A_1 and E frequencies are barely outside the experimental uncertainty. They can be removed by including small additional interaction constants to the force field. The potential energy distribution, shown in Table IV, shows a complete separation of the internal coordinates in the normal

(5) A. Olin, *Acta Chem. Scand.*, **14**, 126, 814, 1999 (1960); *Svensk Kem. Tidskr.*, **73**, 482 (1961).
(6) O. E. Esval and J. S. Johnson, *J. Phys. Chem.*, **69**, 959 (1965).
(7) C. Brosset, *Arkiv Kemi*, **1**, 353 (1949); *Arkiv Kemi, Mineral. Geol.*, **A20**, No. 7 (1945).
(8) E. B. Wilson, J. C. Decius, and P. C. Cross, "Molecular Vibrations," McGraw-Hill Book Co., Inc., New York, N. Y., 1955.
(9) R. G. Snyder and J. H. Schachtschneider, *Spectrochim. Acta*, **19**, 117 (1963).

TABLE II

SYMMETRY COORDINATES FOR $Pb_4(OH)_4^{4+}$ [a]

A_1

$$S_r^{(A_1)} = \frac{1}{\sqrt{12}}[r(1,5) + r(2,5) + r(1,6) + r(2,6) + r(3,5) + r(2,7) + r(4,6) + r(1,8) + r(3,7) + r(4,7) + r(3,8) + r(4,8)]$$

$$S_D^{(A_1)} = \frac{1}{\sqrt{6}}[D(1,2) + D(1,3) + D(1,4) + D(2,3) + D(2,4) + D(3,4)]$$

E

$$S_r^{(E)} = \frac{1}{\sqrt{24}}[2r(1,6) + 2r(2,5) + 2r(3,7) + 2r(4,8) - r(1,5) - r(1,8) - r(2,6) - r(2,7) - r(3,5) - r(3,8) - r(4,6) - r(4,7)]$$

$$S_D^{(E)} = \frac{1}{\sqrt{12}}[2D(1,3) + 2D(2,4) - D(1,4) - D(1,2) - D(2,3) - D(3,4)]$$

F_2

$$S_{r(1)}^{(F_2)} = \frac{1}{\sqrt{12}}[r(1,5) + r(2,5) + r(3,5) + r(4,6) + r(4,7) + r(4,8) - r(1,6) - r(2,6) - r(3,7) - r(3,8) - r(2,7) - r(1,8)]$$

$$S_{r(2)}^{(F_2)} = \frac{1}{\sqrt{6}}[r(1,5) + r(2,5) + r(3,5) - r(4,6) - r(4,7) - r(4,8)]$$

$$S_D^{(F_2)} = \frac{1}{\sqrt{6}}[D(1,2) + D(1,3) + D(2,3) - D(1,4) - D(2,4) - D(3,4)]$$

[a] Symbols: r, D = internal coordinates defined in Figure 1. Numbers in parentheses refer to atoms connected by the internal coordinate, following the numbering system in Figure 1.

TABLE III

SUMMARY OF VIBRATIONAL CALCULATIONS FOR $Pb_4(OH)_4^{4+}$

	Frequencies, cm^{-1}		
Species	Obsd	Calculation I	Calculation II
A_1	404	402	406
	130	125	126
E	455	453	457
	60	65	63
F_2	505	507	503
	346	348	345
	87	90	89
	Force constants, mydn/Å		
K		1.663	1.690
k'		0.135	0.140
k''		−0.106	−0.272
D		0.542	0.528

modes. The four frequencies above 340 cm^{-1} can be attributed entirely to Pb–O stretching while the three frequencies below 140 cm^{-1} can be attributed entirely to Pb–Pb stretching.

Esval's radial distribution curve[4] provides an accurate estimate of the Pb–Pb distance, but the lighter oxygen atoms are located with much less accuracy. In order to assess the effect of this uncertainty on our calculation, a new G matrix was constructed using a Pb–O distance increased by 0.14 Å. This increment corresponds roughly to half of the half-width of the peak assigned to the Pb–O interaction in the radial distribution curve. The results obtained with this revised G matrix and the same force field as before are shown in Table III under calculation II. They are much the same as for calculation I, slight changes in the force constants sufficing to produce an equally good frequency fit.

TABLE IV

POTENTIAL ENERGY DISTRIBUTIONS FOR $Pb_4(OH)_4^{4+}$

Normal mode freq, cm^{-1}	V_{rr} [a]	V_{DD}
505 (F_2)	100	0
455 (E)	100	0
404 (A_1)	99	1
346 (F_2)	100	0
130 (A_1)	1	99
87 (F_2)	0	100
60 (E)	0	100

[a] $V_{i,j}$ = normalized contribution to the potential energy from F matrix elements of the type (i,j).

The Metal Cage Approximation

Because the Pb–O and Pb–Pb internal coordinates are separated essentially completely in the normal modes, the motions of the Pb_4 cage can be considered independently of the oxygen motions. Four like atoms in a tetrahedral array (*cf.* P_4[10]) have three normal modes, of symmetry A_1, F_2, and E. Their symmetry G matrix elements are in the ratio 4:2:1, in the order given. Consequently, if a primary stretching force constant is sufficient to account for the motions, then the corresponding frequencies must be in the ratio $2:\sqrt{2}:1$. $Pb_4(OH)_4^{4+}$ has three low-frequency Raman bands at 130, 87, and 60 cm^{-1}, the highest one being polarized and therefore of A_1 symmetry. They are in the ratio 2:1.32:0.93, and a single Pb–Pb stretching constant was found adequate to calculate all three to reasonable accuracy.

A similar situation was encountered[2] in the case of $Bi_6(OH)_{12}^{6+}$. Here too the separation of Bi–O and Bi–Bi internal coordinates in the normal mode is essentially complete, and the motions of the Bi_6 cage can be considered in isolation. Six like atoms in an octahedral array have three Raman-active modes, of A_{1g}, F_{2g}, and E_g symmetry, and one infrared-active mode, of F_{1u} symmetry. The symmetry G matrix elements for the first three modes are again in the ratio 4:2:1. $Bi_6(OH)_{12}^{6+}$ has three low-frequency Raman bands, at 177, 107, and 88 cm^{-1}, which are in the ratio 2:1.26:1.00. Again a single Bi–Bi stretching constant was found adequate to calculate the three frequencies. (The low-frequency infrared band was unobservable.)

It appears that for tetra- or hexanuclear complexes a diagnostic test for tetrahedral or octahedral cages may be available in the Raman spectrum: namely, the observation at low frequency of three bands, the highest being polarized, whose frequencies fall approximately in the ratio $2:\sqrt{2}:1$.

Vibrational Analysis for $Pb_6(OH)_8^{4+}$

As noted in the Introduction, $Pb_6(OH)_8^{4+}$ is the probable composition of the complex present in concen-

(10) G. Herzberg, "Infrared and Raman Spectra of Polyatomic Molecules," D. Van Nostrand, Princeton, N. J., 1959, p 164.

trated perchlorate solutions containing 1.33 hydroxyls per lead and in crystals obtained therefrom. The most symmetrical structure for this unit would be an octahedral array of lead atoms with hydroxyls on the octahedral faces. The vibrational spectrum[3] was found to be qualitatively consistent with this structure, although others could not be excluded.

In the light of the preceding section it now seems quite significant that the Raman spectrum of the complex in question shows three low-frequency bands, at 142, *ca.* 95, and 68 cm^{-1}, the first one being polarized. These frequencies are in the ratio 2:1.32:0.95. The presumption is strong that we are in fact dealing with an octahedral Pb_6 cage.

Accordingly we felt it worthwhile to perform a normal coordinate analysis on the spectrum, using the proposed octahedral structure. The Pb–Pb and Pb–O distances were assumed to be the same as in $Pb_4(OH)_4^{4+}$. Symmetry coordinates were constructed from the metal–oxygen and metal–metal internal coordinates, which are equivalent respectively to the symmetry coordinates constructed for the angle γ and the metal–metal coordinates in $Bi_6(OH)_{12}^{6+}$.[2]

The six observed frequencies could be adequately reproduced with three force constants: for Pb–Pb stretching (D), Pb–O stretching (K), and stretch–stretch interaction between adjacent Pb–O bonds at Pb (k'). The results are shown in Table V. The potential energy

TABLE V

SUMMARY OF VIBRATIONAL CALCULATIONS FOR $Pb_6(OH)_8^{4+}$

	Frequencies, cm^{-1}		Potential energy distribution for calculation III	
		Calculation		
Species	Obsd	III	V_{rr}[a]	V_{DD}
A_1	386	391	99	1
	142	141	1	99
E	454	451	100	0
	68	71	0	100
F_{2g}	[b]	383	99	1
	[b]	301	100	0
	Ca. 95	96	1	99
F_{1u}	[b]	441	100	0
	365	365	99	1
	[c]	120	1	99

Force constants,[d] mdyn/Å: $K = 1.284$, $k' = 0.192$, $D = 0.645$

[a] $V_{i,j}$ = normalized contribution to the potential energy for F matrix elements of the type (i,j). [b] Not resolved. [c] Not observed. [d] The force constants are defined in the text.

distribution, also given in Table V, again shows almost complete separation of Pb–O and Pb–Pb coordinates in the normal modes. Four of the ten bands expected for this structure were not observed in the vibrational spectra. We now turn to the frequencies predicted for these modes by the calculation. Two of them, at 383 and 301 cm^{-1}, are of F_{2g} symmetry and should be Raman active. The first of these, however, is almost coincident with the strong A_{1g} band at 386 cm^{-1}, and would be completely obscured by it. In the region of 301 cm^{-1} the experimental Raman spectrum (Figure 2 of ref 3) shows a flat region which does appear to have

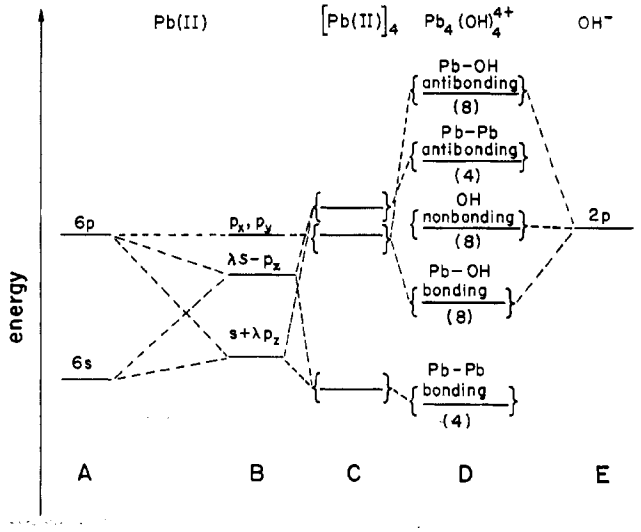

Figure 2.—Qualitative energy level scheme proposed for $Pb_4(OH)_4^{4+}$ (see text). Numbers in parentheses refer to the number of molecular orbitals of each type.

excess emission over the sloping base line. This could arise from the expected F_{2g} mode. The higher frequency triply degenerate modes are quite weak in the Raman spectra of both $Pb_4(OH)_4^{4+}$ and $Bi_6(OH)_{12}^{6+}$.

The remaining two unobserved modes, at 441 and 120 cm^{-1}, are of F_{1u} symmetry and infrared active. The former frequencies lies within the broad infrared band centered at 365 cm^{-1} (Figure 3 of ref 3). This band is split into three components and also shows a weak shoulder at about 450 cm^{-1}. The low-frequency infrared spectrum, where the remaining F_{1u} mode is predicted, shows only very broad absorption.

Discussion

It is evident that the vibrational spectrum of $Pb_4(OH)_4^{4+}$ is in good quantitative accord with the tetrahedral structure proposed by Esval[4] on the basis of the analysis presented here. All seven frequencies are adequately fit with four force constants, and these seem of reasonable magnitude. The Pb–O stretching constant, 1.66 mdyn/Å, is nearly the same as the Bi–O constant, 1.75 mdyn/Å, in $Bi_6(OH)_{12}^{6+}$ (*vide infra*). The stretch–stretch interaction constants are less than 10% of the primary stretching constant. As in the case of $Bi_6(OH)_{12}^{6+}$ we note that the effect of variation in the uncertain oxygen positions is mainly taken up by the interaction constants, and the primary force constants are little influenced.

In the case of $Bi_6(OH)_{12}^{6+}$ it proved efficient to substitute a metal–metal stretching coordinate and force constant for bond bending, and a dramatic improvement of the separation of the internal coordinates in the normal modes resulted. For $Pb_4(OH)_4^{4+}$ it was impossible to obtain an adequate fit of the data with a limited number of reasonable force constants, if only Pb–O interactions were considered. Inclusion of metal–metal stretching in place of bond bending gave a calculation quite as satisfactory as for $Bi_6(OH)_{12}^{6+}$. It is possible that the simplification is artificial and that inclusion of metal–metal stretching merely masks real

complications in the force field. However, it would seem a remarkable coincidence if this were simultaneously the case for two such different structures as $Bi_6(OH)_{12}^{6+}$ and $Pb_4(OH)_4^{4+}$.

In any event our main argument for some degree of metal–metal bonding rests, as in the case of $Bi_6(OH)_{12}^{6+}$, on the fact that the three low-frequency bands associated exclusively with motions of the metal atoms have the highest intensity in the Raman spectrum. Large polarizability changes for these modes would be expected if electrons are to some extent delocalized in the metal cage. If, on the other hand, the bonding electrons are entirely localized between the lead and oxygen atoms, one would expect the high-frequency, primarily Pb–O stretching, modes to have higher polarizability changes and intensities.

The metal–metal distance is slightly larger in $Pb_4(OH)_4^{4+}$ than in $Bi_6(OH)_{12}^{6+}$ (3.83 *vs.* 3.71 Å), and this may be one factor in the former having a 50% smaller metal–metal stretching constant (0.54 *vs.* 0.96 mdyn/Å). On the other hand the Pb–Pb distance is only 0.33 Å longer than the internuclear distance in metallic lead, as compared to a 0.61-Å difference in the case of bismuth.

The vibrational analysis for the presumed $Pb_6(OH)_8^{4+}$ must be considered speculative in the absence of any structural data. Nevertheless the results are striking. A very simple force field in conjunction with the proposed octahedral structure accounts quite adequately for all of the spectral features. The observation of the three intense low-frequency Raman bands at their characteristic frequency ratios suggests at the least that we are dealing with a lead cage of cubic symmetry. A crystallographic structure determination of this complex will hopefully provide a critical test of this diagnostic use of the Raman spectrum. If the analysis turns out to be based on the correct structure, it suggests that conversion of $Pb_4(OH)_4^{4+}$ to $Pb_6(OH)_8^{4+}$ is accompanied by a 20% increase in the Pb–Pb stretching constant, D. It should be noted that the calculation of D is independent of the assumed molecular parameters in the metal cage approximation. The Pb–O stretching constant, K, on the other hand, is observed to decrease by about 30%, but the calculation of K is somewhat dependent on the oxygen positions (*cf.*, calculations I and II for $Pb_4(OH)_4^{4+}$) which are, of course, unknown for $Pb_6(OH)_8^{4+}$.

We now turn to the question of whether metal–metal bonding can be considered a reasonable feature of the electronic structure of these lead(II) polyhedra. The Pb–Pb distance in $Pb_4(OH)_4^{4+}$, 0.33 Å longer than in the metal, may still be short enough to allow some overlap of atomic orbitals. The bonding under consideration is quite weak. As in the case of $Bi_6(OH)_{12}^{6+}$ we choose sp_z hybrids (z taken as the direction on each lead toward the center of the cage) as the likeliest candidates for overlap and leave p_x and p_y orbitals for bonding to hydroxide.

The result for $Pb_6(OH)_8^{4+}$ is the same as for $Bi_6(OH)_{12}^{6+}$: six bonding orbitals inside the cage, in which the metal valence electrons could be delocalized, and six antibonding orbitals outside the cage. There are twelve metal–oxygen bonding orbitals accommodating 24 electrons from hydroxide. In the case of $Pb_6(OH)_8^{4+}$ these are provided by eight hydroxides instead of twelve, and a total of twelve filled hydroxide orbitals are left nonbonding instead of 24. An energy level diagram for $Pb_6(OH)_8^{4+}$ on this scheme would differ from that of $Bi_6(OH)_{12}^{6+}$ (Figure 2 of ref 2) only in the number of hydroxide nonbonding orbitals. This arrangement of orbitals is still equivalent to a set of twelve three-center two-electron O–M–O bonds, and the average M–O bond order is still one-half.

For $Pb_4(OH)_4^{4+}$ the same bonding scheme produces four bonding metal–metal orbitals, accommodating the eight lead valence electrons. There are eight metal–oxygen bonding orbitals available for sixteen hydroxide electrons, leaving one filled orbital on each hydroxide nonbonding. A possible energy level scheme, closely similar to that for $Bi_6(OH)_{12}^{6+}$, is shown in Figure 2. As in the case of $Bi_6(OH)_{12}^{6+}$ we stress that the ordering of the levels is not unambiguous and that the diagram merely serves to show that weak metal–metal bonding can be reasonably taken into account. The orbital arrangement is now equivalent to four four-center four-electron O_3Pb (or OPb_3) bonds, and the average Pb–O bond order is two-thirds. The apparent decrease in the M–O stretching constant between $Pb_4(OH)_4^{4+}$ and $Pb_6(OH)_8^{4+}$ may then reflect the higher bond order of the former. On the other hand the observation that $Bi_6(OH)_{12}^{6+}$ has essentially the same M–O stretching constant as does $Pb_4(OH)_4^{4+}$ suggests that the decrease in bond order is in this case balanced by the increase in nuclear charge on the metal.

Acknowledgment.—This work made use of computer facilities supported in part by National Science Foundation Grant NSF GP 579.